

pH-Induced Changes in Activity and Conformation of NADH Oxidase from *Thermus thermophilus*

G. ŽOLDÁK¹, A. MUSATOV², M. STUPÁK^{1*}, M. SPRINZL³ AND E. SEDLÁK¹

¹ Department of Biochemistry, Faculty of Science, P. J. Šafárik University, Košice, Slovakia. E-mail: zoldakg@yahoo.co.uk

² Department of Biochemistry, The University of Texas Health Science Center, San Antonio, Texas, 78229–3900, U.S.A.

³ Laboratorium für Biochemie, Universität Bayreuth, Germany

Abstract. *Thermus thermophilus* NADH oxidase (NOX) activity exhibits a bell-shaped pH-dependency with the maximal rate at pH 5.2 and marked inhibition at lower pH. The first pH transition, from pH 7.2 to pH 5.2, results in more than a 2-fold activity increase with protonation of a group with $pK_a = 6.1 \pm 0.1$. The difference in fluorescence of the free and enzyme-bound flavin strongly indicates that the increase in enzyme activity in a pH-dependent manner is related to a protein-cofactor interaction. Only one amino acid residue, His75, has an intrinsic $pK_a \sim 6.0$ and is localized in proximity ($<10 \text{ \AA}$) to N5-N10 of the isoalloxazine ring and, therefore, is able to participate in such an interaction. Solvent acidification leads to the second pH transition from pH 5.2 to 2.0 that results in complete inhibition of the enzyme with protonation of a group with an apparent $pK_a = 4.0 \pm 0.1$. Inactivation of NOX activity at low pH is not caused by large conformational changes in the quaternary structure as judged by intrinsic viscosity and sedimentation velocity experiments. NOX exists as a dimer even as an apoprotein at acidic conditions. There is a strong coupling between the fluorescence of the enzyme-bound flavin and the intrinsic tryptophans, as demonstrated by energy transfer between Trp47 and the isoalloxazine ring of flavin adenine dinucleotide (FAD). The pH-induced changes in intrinsic tryptophan and FAD fluorescence indicate that inhibition of the FAD-binding enzyme at low pH is related to dissociation of the flavin cofactor, due to protonation of its adenine moiety.

Key words: NADH oxidase — Flavoproteins — Viscosity — Enzyme activation — Thermophile enzymes

Correspondence to: Erik Sedlák, Department of Biochemistry, Faculty of Science, P. J. Šafárik University, Moyzesova 11, 040 01 Košice, Slovakia. E-mail: sedlak_er@saske.sk

* Present address: Department of Medical Chemistry and Biochemistry, Medical Faculty, P. J. Šafárik University, Trieda SNP 1, 040 66 Košice, Slovakia

Introduction

NADH oxidase (NOX) (EC 1.6.99.3.) from *Thermus thermophilus* is a homodimeric flavoprotein containing 1 molecule of flavin mononucleotide (FMN) (or flavin adenine dinucleotide (FAD)) *per* ~25-kDa monomer. The enzyme catalyzes hydride transfer from NADH to an acceptor such as FAD, ferricyanide, oxygen, and others. A physiological role of this “alternative” dehydrogenase in the thermophile species is not known, but it has been recently reported that some NOX and homologous nitroreductases might contribute to the defenses against oxidative stress (Liochev et al. 1999; Ward et al. 2001; Koder et al. 2002; Kengen et al. 2003).

The known crystal structure of NOX, the high stability of the protein and the tight interaction of the flavin cofactor with the enzyme (Hecht et al. 1995) make this protein interesting for investigating the factors that affect the activity of the enzyme, especially the protein-flavin interaction (Žoldák et al. 2003, 2004). The results of such studies could be generally applied to the family of NOX because they all share a similar quaternary structure, folding pattern and key amino acids with several flavin-containing nitroreductases (Parkinson et al. 2000; Kobori et al. 2001; Haynes et al. 2002). Moreover, the ability of nitroreductases to convert relatively non-toxic prodrugs into highly cytotoxic derivatives makes this protein family attractive for its potential for cancer gene therapy.

Lowering the pH increase the catalytic rate of the enzyme (Park et al. 1992). This was an unexpected result since deprotonated flavin was believed to be a better reductant (Su and Klinman 1999). The question remains of which enzyme component is responsible for pH-induced activation: is it an amino acid residue(s) and/or the flavin cofactor? In an effort to answer this question, biophysical and biochemical approaches were applied in this study.

Very recently, we have shown that NOX from *T. thermophilus* is activated by a low concentration of denaturant (urea, guanidium hydrochloride (GdmHCl)) and that enzyme activity is extremely sensitive to anions of the Hofmeister series (Žoldák et al. 2003, 2004). These findings were interpreted as the effect of modified dynamics of the enzyme active site. Therefore, the question remains whether pH-induced activation is analogously related to a change in dynamics of the active site as was observed in the presence of urea (Žoldák et al. 2003)?

In the present work we studied structural and functional changes of NOX caused by pH. We observed an increased catalytic rate of NOX that is directly linked to the protein-cofactor interaction. This work also confirms our previous suggestion that activation of the enzyme, at least partially, results from destabilization of the enzyme's active site.

Materials and Methods

Urea (high purity grade) was purchased from Sigma. The concentration of urea was determined from refractive index using an Abbe Refractometer AR3-AR6. The pH of the solutions was measured at room temperature with a Sensorex glass

pH electrode before and after each experiment. The pH values were corrected for the presence of denaturant (Garcia-Mira and Sanchez-Ruiz 2001; Acevedo et al. 2002). Other chemicals were of analytical grade.

Protein expression and purification

The purification procedure for the overproduced NOX has been described earlier (Park et al. 1992) and was used in the present work with minor modifications (Žoldák et al. 2003). Protein purity was analyzed by SDS-PAGE stained with Coomassie Brilliant Blue (Laemmli 1970). Three different preparations of NOX were used in our current work. All experiments were performed in triplets. All obtained enzymes showed very similar specific activity and similar trends in pH dependent activity. The final preparation yielded NOX with a specific activity of 11.32 units/mg measured in 50 mmol/l phosphate buffer, pH 7.2. One unit is defined as 1 $\mu\text{mol/l}$ NADH oxidized/min. The protein concentration with the bound cofactor was determined using the extinction coefficient $\varepsilon_{280} = 51,560 \text{ (mol/l)}^{-1} \cdot \text{cm}^{-1}$ (Pace et al. 1995; Žoldák et al. 2003).

Steady-state kinetics

All kinetic measurements were performed on a UV 3000 spectrophotometer (Shimadzu). The kinetic parameters were determined from the initial decrease in NOX absorbance at 340 nm ($\varepsilon_{340} = 6220 \text{ (mol/l)}^{-1} \cdot \text{cm}^{-1}$ (Dawson et al. 1986)), at 20°C. Measurements were performed after 1 h incubation of 120 nmol/l NOX in buffer with appropriate pH, containing 0.120 mmol/l FAD ($\varepsilon_{375} = 9300 \text{ (mol/l)}^{-1} \cdot \text{cm}^{-1}$ (Dawson et al. 1986)). 50 mmol/l sodium acetate buffer was used in the pH range of 4.5–6.0; 50 mmol/l sodium phosphate buffer was used in the pH range of 2.0–4.5 and 5.5–8.5; 50 mmol/l glycine buffer was used in the pH range of 8.0–10.0. NADH self-decay rate was measured under the same conditions, but without enzyme. The self-decay of NADH was taken into account only at high temperatures and low pH.

Temperature-dependence of enzymatic activity

The enzymatic activity *vs.* temperature was measured in 50 mmol/l phosphate buffer, containing 0.120 mmol/l of FAD and 120 nmol/l of enzyme. The reaction was started by addition of NADH to a final concentration of 0.180 mmol/l. The assay was performed within the temperature range of 20–50°C. The temperature ($\pm 0.3^\circ\text{C}$) was controlled by a digital thermometer connected to a computer.

Experimental data were analyzed using the Arrhenius equation:

$$\ln k_{\text{cat}} = -\frac{E_a}{RT} + C_1 \quad (1)$$

where, k_{cat} is initial velocity of NADH oxidation, R is the gas constant, T is the absolute temperature, E_a is the activation energy for the observed reaction and C_1 is a temperature independent constant. Data (at least 5 points) were plotted as $\ln k_{\text{cat}}$ *vs.* T^{-1} and analyzed by linear regression. Linearity of Arrhenius plot indicated that the Arrhenius equation was a sufficient descriptor of the temperature

dependence of enzyme activity. Only Arrhenius plots with coefficients of linearity greater than 0.98 were used. Coefficients of linearity lower than 0.98 led to high standard deviations (S.D.) of the apparent activation energies relative to the magnitude of the observed effect. Errors were calculated from a linear fitting procedure and showed how the Arrhenius equation described the experimental data. Linear data fitting results in the line's intercept and slope \pm S.D. The activation parameters were determined in the range of pH 5 to 10. A comparison of the Arrhenius equation and the transition state theory, the enthalpy (ΔH^*) and entropy (ΔS^*) of activation were calculated using the following equations:

$$\Delta H^* = E_a - R \cdot T \quad (2)$$

$$T \cdot \ln \left(\frac{k_{\text{cat}}}{T} \right) = \frac{T \cdot \Delta S^*}{R} + C_2 \quad (3)$$

C_2 is the temperature independent constant. This approach avoided any long extrapolation connected with large errors in the estimation of the activation entropy (Cornish-Bowden 2002).

Fluorescence emission spectroscopy

The fluorescence steady state measurements were done on a RF 5000 spectrofluorometer (Shimadzu). Using different excitation wavelengths, i.e. 290 and 450 nm, we could follow changes in the environment close to different internal chromophores, i.e. tryptophan and FAD, respectively. The cuvette contained the given buffer and 2.4 $\mu\text{mol/l}$ protein in a total volume of 2.5 ml, at 20°C. The pH of the assayed mixture was adjusted by addition of small aliquots of HCl or NaOH.

Analysis of the titration curve

pH dependence of fluorescence, ellipticity and activity were satisfactorily fitted to the following equation based on a two state model. The measured signal (S) was analyzed by:

$$S = \left[\frac{y_L + y_U \cdot 10^{n(\text{p}K_a - \text{pH})}}{1 + 10^{n(\text{p}K_a - \text{pH})}} \right] \quad (4)$$

where y_L and y_U are the lower and upper limits of the measured parameter, respectively, and n is the number of protons involved in the transition. The slopes and intercepts of the pH dependence of the pre- and post-transition region have been taken into account to correct the experimental data.

Circular dichroism measurements

Circular dichroism measurements were performed on an Olis Cary-16 (USA) and a Jasco J-810 (Japan) spectropolarimeter using 29.3 $\mu\text{mol/l}$ NOX in 10 mmol/l sodium phosphate buffer at various pH. A 0.1-cm path length cuvette was used for scanning the peptide region and a 1-cm cuvette was used for the aromatic region. Each spectrum represents an average of the accumulation of 4–6 consecutive scans.

The temperature was kept constant at 20°C by a temperature-controlled water bath circulation.

Heat-induced conformational transitions of NOX measured by circular dichroism were recorded in a Jasco J-810 spectropolarimeter equipped with a PTC-423S/L Peltier element. Protein concentration was $\sim 5 \mu\text{mol/l}$ in 50 mmol/l phosphate (pH range 8.0–5.8) or 50 mmol/l acetate buffer (pH range 2.0–5.8) at each given pH. The scan rate was 1 K/min.

Viscosimetry

All viscosimetric measurements were performed on a VISCODENS using a defined shear rate γ of 60 s^{-1} (Bánó et al. 2003). The volume of the sample was 1.6 ml. Samples were dialyzed overnight against 50 mmol/l sodium phosphate buffer, pH 7.5, 5.5 and 3.2 and against 50 mmol/l sodium phosphate buffer, pH 7.5, containing 6.0 mol/l GdmHCl. The specific viscosity was calculated using the following equation:

$$\eta_{\text{spec}} = \frac{\eta - \eta_0}{\eta_0} \quad (5)$$

where η is the relative viscosity of the protein and η_0 is the relative viscosity of the reference buffer. The reduced viscosity η_{red} [ml/g] can be calculated by applying the following equation:

$$\eta_{\text{red}} = \frac{1}{c} \times \eta_{\text{spec}} \quad (6)$$

where c is the concentration of the protein in g/ml. The intrinsic viscosity was usually determined from linear extrapolation of the reduced viscosities at five different concentrations of protein

$$[\eta] = \lim_{c \rightarrow 0} \eta_{\text{red}} \quad (7)$$

Analytical ultracentrifugation

Sedimentation experiments were performed in the Center for Analytical Ultracentrifugation of Macromolecular Assemblies located in the Department of Biochemistry at The University of Texas Health Science Center at San Antonio, U.S.A. (<http://www.cauma.uthscsa.edu>). Sedimentation velocity and equilibrium runs were carried out in a Beckman XL-A analytical ultracentrifuge. Sedimentation velocity was done at 50,000 and 60,000 rpm for the samples with and without GdmHCl, respectively. Data has been collected at 280 nm at 20°C. Sedimentation equilibrium was performed at 38,000, 42,000 and 46,000 rpm using a rotor AN 60 at 20°C. Sedimentation equilibrium data of NOX at three different concentrations of protein (4.85, 6.6 and 8.73 $\mu\text{mol/l}$) were collected at 280 nm at 4°C. Best fits were obtained assuming a single component species. Both sedimentation equilibrium and sedimentation velocity data were analyzed using the UltraScan (version 6.2.0.) computer software (<http://www.ultrascan.uthscsa.edu>) as previously described (Musatov et al. 2000). The partial-specific volume of the protein and the

buffer density and viscosity were calculated using the same program. Prior to sedimentation analysis, samples were dialyzed overnight at 4°C against appropriate buffer.

Fraction calculation of different protonated states of the enzyme

We assumed that protons bind independently to the enzyme. The partition function (P) for the independent binding is given by (Wyman and Gill 1990)

$$P = \prod_{i=1}^n (1 + K_{a,i} [H^+])$$

where $K_{a,i}$ is the individual single site binding constant. For two binding sites

$$P = 1 + \underbrace{(K_{a,1} + K_{a,2})}_{f_0} [H^+] + \underbrace{(K_{a,1} \times K_{a,2})}_{f_1} [H^+] + \underbrace{(K_{a,1} \times K_{a,2})}_{f_2} [H^+]^2$$

The fraction of species α_i of macromolecules with/without protons bound is equal to

$$\alpha_i = \frac{f_i}{P} \quad (8)$$

where $\sum_{i=0}^N \alpha_i = 1$. The dependence of activity (A_{obs}) on pH was calculated according to

$$A_{\text{obs}} = \sum_{i=0}^N \alpha_i A_i \quad (9)$$

where A_i is the activity of the given fraction.

Results

Effect of pH on activity, activation parameters and intrinsic fluorescence of NOX

The decrease of pH from 7.0 to 5.0 resulted in more than a 2-fold increase in activity. The maximum activity was observed at pH 5.2 (Figure 1A). The pH-dependent activity in the region of neutral to acidic pH had a sigmoidal character with an apparent $pK_a = 6.1 \pm 0.1$. A further decrease in pH from 7.0 to ~ 5.2 caused an increase in k_{cat} and an apparent Michaelis constant ($K_{M,\text{app}}$) from 6.6 s^{-1} to 17.4 s^{-1} and from 5.3 to $7.7 \text{ }\mu\text{mol/l}$, respectively (Table 1). These values are in good agreement with previously reported kinetic parameters at neutral pH (Park et al. 1992). After reaching the maximum, further acidification resulted in a sigmoidal shaped decrease in activity (Figure 1A). At very acidic pH, a significant increase in the nonenzymatic decay of NADH was observed in contrast with a decrease in the enzymatic NADH oxidation. The pH dependence of the enzyme activity in the

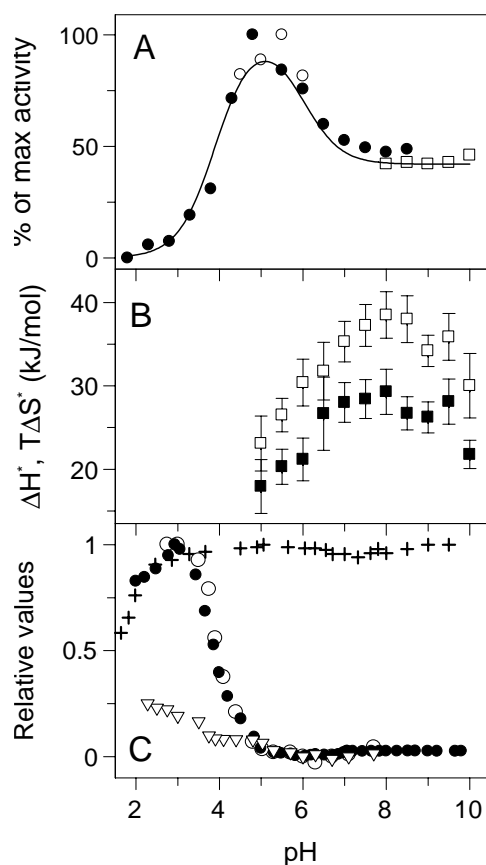


Figure 1. pH dependence of activity, thermodynamic and structural parameters of NOX. **A.** The effect of pH on the activity of the FAD form of NOX from *T. thermophilus*. Different symbols designate different buffers used in the given pH range: glycine, 8.0–10.0 (\square); sodium phosphate, 5.5–8.5, 2.0–4.5 (\bullet); sodium acetate, 4.5–6.0 (\circ). Values are shown as percents of maximal activity value at pH \sim 5. The theoretical curve was calculated according to Eq. (9), where activity of the unprotonated enzyme was 40% of the protonated enzyme (100%), and the activity of the double protonated enzyme was 0%. **B.** Activation parameters ΔH^* (\square) and $T\Delta S^*$ (\blacksquare) at 20°C as a function of pH. Values were obtained from kinetic experiments described in Materials and Methods using Eqs. (1–3). Arrhenius plots were analyzed at various pH and temperatures in the range from 20°C to 40°C. Errors were calculated according to deviation from linearity of the Arrhenius plots. Activation parameters are not shown at pH $<$ 4.5 because of the large error of evaluation due to increased nonenzymatic oxidation of NADH. **C.** The pH dependence of relative values (related to maximal values) of intrinsic tryptophan fluorescence of NOX (\bullet), fluorescence of N-acetyl-L-tryptophanamide, an analogue of tryptophan residues in protein completely exposed to molecules of solvent (+), ellipticity in the aromatic region at 265 nm (\circ), and in the peptide region at 220 nm (∇) of the FAD form of NOX from *T. thermophilus*. Tryptophan fluorescence was monitored at 344 nm using an excitation wavelength of 290 nm.

acidic area corrected for the nonenzymatic reaction had a sigmoidal shape with an apparent $pK_a = 4.0 \pm 0.1$. When the pH was decreased from 10.0 to \sim 7.0, there were no significant changes in NOX activity.

To determine the activation parameters of NOX, enzyme activity was measured over a temperature range of 20 to 40°C and was calculated according to Eqs. (1–3). The obtained data show that acidification leads to a decreased activa-

Table 1. Catalytic rate, Michaelis constant and their ratios at various pH at 20 °C

| pH | k_{cat} (s^{-1}) | $K_{\text{M,app}}$ ($\mu\text{mol/l}$) | $k_{\text{cat}}/K_{\text{M,app}}$ ($10^6 (\text{mol/l})^{-1}\text{s}^{-1}$) |
|-------|---|---|--|
| 10.00 | 5.6 | 7.2 | 0.78 |
| 8.50 | 6.2 | 5.4 | 1.15 |
| 7.00 | 6.6 | 5.3 | 1.25 |
| 5.50 | 17.4 | 7.7 | 2.26 |
| 4.00 | 8.1 | 8.0 | 1.01 |
| 2.50* | 1.5 | n.d. | n.d. |

n.d., not determined; * affected by large errors due to the high decay rate of NADH.

tion entropy and enthalpy of the enzyme-catalyzed NADH oxidation (Figure 1B). The activation parameters at very acidic pH are not shown since their determination was significantly affected by the nonenzymatic oxidation of NADH and the non-linearity of the Arrhenius plots (for details see Materials and Methods).

The intrinsic tryptophan fluorescence increased in a sigmoidal way with acidification of the solvent, apparent $\text{p}K_{\text{a}} = 3.80 \pm 0.05$. However, the fluorescence of N-acetyl-L-tryptophanamide, which is an analogue of tryptophan residues in protein exposed to solvent, did not show a pH-induced transition in the pH range from 2 to 10 (Figure 1C). The effect of acidification on the protein was also monitored following changes in ellipticity in the aromatic region of the enzyme. The observed pH-induced transition was characterized by $\text{p}K_{\text{a}} = 4.02 \pm 0.15$ (Figure 1C). The intense positive signal at 265 nm disappeared at $\text{pH} < 2$ indicating changes near the flavin cofactor and tryptophan residues. In fact, the pH-induced inhibition of NOX was accompanied by dissociation of the cofactor during dialysis. The ellipticity at 222 nm decreased by 25% at $\text{pH} \sim 2.3$, suggesting the high stability of the enzyme's secondary structure.

It should be noted that the maximum activity at $\text{pH} \sim 5.2$ was not well-defined in the tryptophan fluorescence or in the ellipticity of the protein (Figure 1C). This is quite unexpected because both tryptophan fluorescence and ellipticity in the aromatic region reflect changes in the environment near the intrinsic probes, i.e. changes in the active site that should accompany the increased enzyme activity.

Structure of the NOX active site

The pH-dependent fluorescence increase in the enzyme's bound flavin is characterized by transitions. The first, or main transition, is well-defined and has a $\text{p}K_{\text{a}} = 3.94 \pm 0.09$ (Figure 2). The second transition is characterized by much smaller fluorescence changes forms a shoulder within the main transition with a $\text{p}K_{\text{a}} = 5.91 \pm 0.10$. However, this shoulder becomes more pronounced in the presence of 1 or 2 mol/l urea (Figure 2). Recently we have shown that a low concentration of urea perturbs the NOX active site (Žoldák et al. 2003). The loosening of the fixed position of the isoalloxazine ring may result in closer contact with the

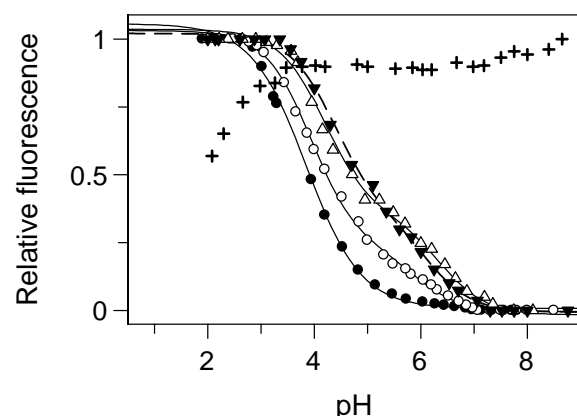


Figure 2. pH dependence of fluorescence of free cofactors and enzyme-bound FAD. The pH dependences of free FAD (●) and FMN (+) in solvent, and enzyme bound FAD in 0 mol/l (○), 1 mol/l (△), 2 mol/l (▼) urea. The curves represent fitted dependence with pK_a values listed in Table 2. The free cofactors and enzyme-bound FAD fluorescence was monitored at 524 and 522 nm, respectively, using an excitation wavelength of 450 nm. All experiments were performed at 20°C.

amino acid residues on its *si*-side. A slight shift of the pK_a to higher pH values indicates a strengthening of this interaction (Table 2). The apparent pK_a of the pH-induced fluorescence increase in the free FAD cofactor was 3.75 ± 0.04 . In contrast to the pH-dependent fluorescence changes of the flavin bound to the enzyme, free FMN did not have a pH-induced transition in this pH range (Figure 2). These data strongly indicate an effect of the adenine moiety on the observed pH-induced transition. Values of the pK_a constants and the number of protons that were involved in the observed pH-induced transitions are summarized in the Table 2.

Interaction between Trp47 and FAD

Identical pK_a constants for the transitions of the tryptophan residues and the flavin cofactor (Table 2) suggest an energy transfer between some of the tryptophan residues and FAD. There is a very good correlation between the fluorescence of these intrinsic probes (Figure 3A). In the presence of 1 to 2 mol/l urea, the correlations were poor (the correlation coefficient $r = 0.796$ and 0.611 , respectively) between flavin and tryptophan fluorescence. These correlations indicate a less efficient energy transfer due to increased dynamics and/or distance between the probes in the active site (Figure 3B). NADH oxidase from *T. thermophilus* contains 4 tryptophan residues. One tryptophan residue, Trp47, located in the enzyme active site, is close enough, ~ 7.7 Å, to interact with the flavin cofactor but only if the enzyme is dimeric (Žoldák et al. 2003). Moreover, the crystal structure reveals that contact between Trp47 and the FAD cofactor is mediated through a tightly bound structural water molecule (Hecht et al. 1995) (Figure 4). This interaction probably results in an intense band at 265 nm and a negative Cotton effect at 285 nm in the near-UV circular dichroism spectrum of NADH oxidase (Žoldák et al. 2003).

Inactivation of NOX at low pH was accompanied by: i) an increase in fluo-

Table 2. Values of pK_a constants and number of protons, n , involved in the pH-induced transitions of NOX and free FAD at various concentrations of urea. Standard deviations with errors were calculated by nonlinear fitting

| Fluorescence | | | | | | |
|-----------------------|---------------------|------------------|--|--|---|--|
| excitation wavelength | emission wavelength | probe | pK_a n | | | |
| | | | 0 mol/l | 1 mol/l | 2 mol/l | |
| 290 nm | 344 nm | tryptophans | 3.90 ± 0.03 1.4 ± 0.1 | n.o. | n.o. | |
| 450 nm | 522 nm | enzyme-bound FAD | $5.91 \pm 0.10^*$ $3.94 \pm 0.09^*$ | $6.38 \pm 0.14^*$ $4.15 \pm 0.10^*$ | $6.12 \pm 0.10^*$ $4.38 \pm 0.10^*$ | |
| 450 nm | 524 nm | FAD | 3.85 ± 0.07 | 3.81 ± 0.08 | 3.90 ± 0.05 | |
| | | | free in solution | 0.90 ± 0.04 | 1.3 ± 0.1 1.1 ± 0.1 | |
| Ellipticity | | | | | | |
| | | | aromatic region | 4.02 ± 0.15 | n.d. n.d. | |
| Activity | | | | | | |
| | | | active site | 6.1 ± 0.1 1.2 ± 0.2 4.0 ± 0.4 1.6 ± 0.2 | 6.2 ± 0.1 1.0 ± 0.2 4.11 ± 0.5 2.0 ± 0.4 | 6.5 ± 0.1 0.8 ± 0.1 4.3 ± 0.7 2.4 ± 0.6 |

n.o., not observed; n.d., not determined; * result of fit of a three-state transition. To reduce free parameters, the value n was constantly 1.

rescence of the intrinsic tryptophans and the flavin cofactor; ii) a decrease in the Cotton effect in the aromatic region of the CD spectrum; and iii) a decrease in ellipticity of $\sim 25\%$ in the peptide region (Figures 1C and 2). These observations and the fact that dialysis of NOX against buffer with pH ~ 3 for 12–15 h at 4 °C produce a colorless enzyme, support the idea that dissociation of the flavin from the enzyme occurs at low pH. Moreover, the temperature of the thermal transition of NOX, as observed by ellipticity at 222 nm, demonstrated decrease in sigmoidal dependence with an apparent pK_a 4.23 ± 0.05 (Eq. (4), Figure 5). This is exactly the effect that would be expected if the cofactor dissociated from the protein. The localization of the flavin cofactor at the dimeric interface suggests the possibility that FAD dissociation may affect the quaternary structure of the enzyme.

Quaternary structure of the apoform of NOX at acidic pH

The integral distribution of the sedimentation coefficients corrected for density and viscosity at 20 °C ($s_{20,w}$) of NOX in 50 mmol/l phosphate buffers with pH

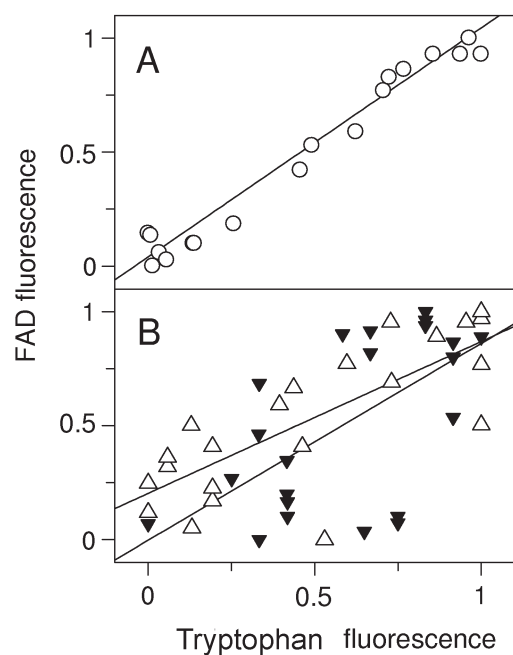


Figure 3. Correlations between FAD fluorescence and intrinsic tryptophans: 0 mol/l (A), and 1 mol/l and 2 mol/l urea (B). Strong linear correlation ($r = 0.953$) between the fluorescence of FAD and the intrinsic tryptophan, Trp47, in the absence of urea (A) indicates energy transfer between Trp47 and FAD. The active site interaction is perturbed in the presence of low concentrations of urea as demonstrated by the correlation coefficients at 1 mol/l and 2 mol/l urea, i.e. 0.796 and 0.611, respectively (B).

Table 3. Intrinsic viscosity and sedimentation coefficient of NOX from *T. thermophilus* at various solvent conditions

| Solvent conditions | Intrinsic viscosity $[\eta]$ ml/g | Svedberg coefficient $s_{20,w}$ |
|------------------------|-----------------------------------|---------------------------------|
| pH 7.5 | 5.83 | 3.05 |
| pH 5.5 | 5.98 | 3.05 |
| pH 3.2 | 6.07 | 3.20 |
| GdmHCl 6 mol/l, pH 7.5 | 22.07* | 1.50 |

* Intrinsic viscosity $[\eta]$ could be calculated from Tanford equation (Tanford et al. 1966): $[\eta] = 0.77 n^{0.666} = 26.68$ ml/g.

7.5, 5.5 and 3.2 was nearly identical and homogeneous with $s_{20,w}$ of 3.0–3.2 S (Figure 6). Clearly, pH did not perturb the oligomeric state of NOX. Sedimentation velocity data of NOX in buffer containing 6.0 mol/l GdmHCl (Figure 6, empty circles) yields the sedimentation coefficient of $s_{20,w} = 1.5$ S. These results suggest that GdmHCl significantly affects the quaternary structure of NOX. To accurately determine molecular weight, NOX in 50 mmol/l buffer (pH 7.5) was analyzed by sedimentation equilibrium. Sedimentation equilibrium data could only be fitted to a single component model of molecular weight $\sim 44,260$ Da (data not shown). The

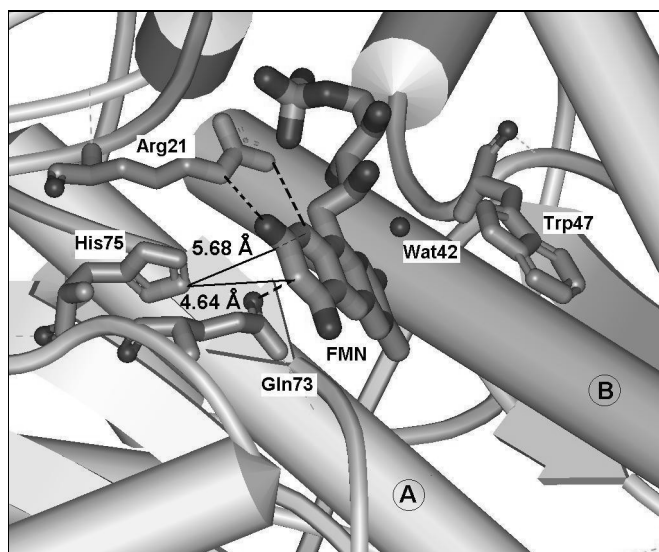
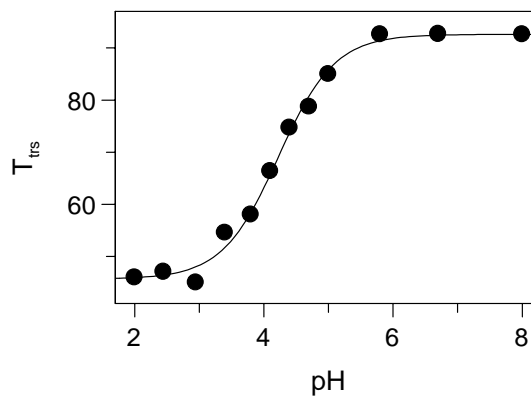


Figure 4. Detailed look at the active site of NOX. The location of FMN, Arg21, His75, Gln73, Trp47 and Wat42 in the dimeric interface of NOX from *T. thermophilus*. The two monomers are designated by the letters A and B. Arg21 and Gln73 create hydrogen bonds with N1, O2 and N3 of the isoalloxazine ring, respectively. His75 is the only histidine within 10 Å from N1 and N3 of the flavin cofactor. Trp47 and the cofactor are intermediated through the tightly bound structural water molecule Wat42. The structure was drawn using Viewer Lite 42 (pdb entry: 1NOX).

Figure 5. Dependence on pH of NOX apparent temperature of thermal transition. Thermal transitions were measured by following ellipticity change at 222 nm. In all cases, the NOX concentration was 5 $\mu\text{mol/l}$. The buffer used was 50 mmol/l phosphate buffer at $\text{pH} > 5.8$ and 50 mmol/l acetate buffer at $\text{pH} < 5.8$. In all cases, the rate scan of heating was 1 K/min. Apparent transition temperatures (T_{trs}) were obtained from nonlinear curve fitting of the two-state transition. In all cases thermal transitions were irreversible. The curve is the fit according to Eq. (4) with $\text{p}K_{\text{a}} = 4.23 \pm 0.05$, $n = 1$.



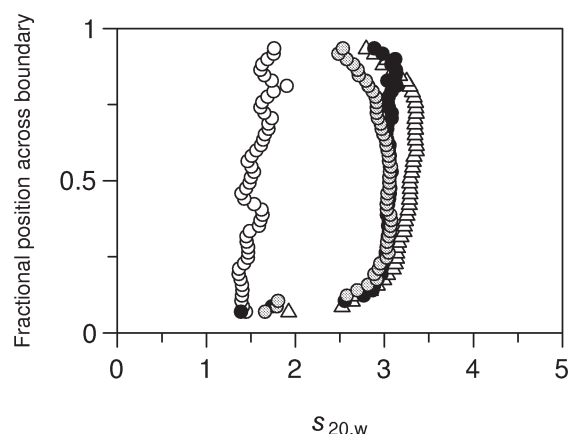


Figure 6. Sedimentation velocity analysis of NOX. Each line represents the distribution of sedimentation coefficients at fractional positions across the sedimenting boundary. Samples of the enzyme were prepared in 50 mmol/l sodium phosphate buffer, pH 7.5 (filled circles), pH 5.5 (grey circles) and pH 3.2 (empty triangles) and run at 60,000 rpm. A sample of NOX in buffer with 6.0 mol/l urea (open circles) was run at 50,000 rpm. The resulting 280 nm absorbance data were analyzed as described in Materials and Methods.

value of 44,260 Da agrees very well with a molecular mass calculated from amino acid sequence of dimeric NOX (Hecht et al. 1995). Therefore, a sedimentation coefficient of ~ 3.0 S is consistent with a dimeric enzyme. It is also reasonable to assume that GdmHCl-treated NOX with $s_{20,w} = 1.5$ S could be assigned to the unfolded monomeric enzyme.

The intrinsic viscosities of NOX at different pH were compared with that of the chemically unfolded enzyme in the monomeric form. The intrinsic viscosity of the enzyme at pH 3.2–7.5 is about 3.8 times lower than the chemically unfolded NOX. These data suggest that the quaternary structure of the enzyme is intact in the pH range of 3.2–7.5 (Table 3). As has been demonstrated by Tanford (Tanford et al. 1966; Tanford 1968), proteins in 6 mol/l GdmHCl are close to the random coil state. The experimentally obtained intrinsic viscosity of NOX in 6 mol/l GdmHCl is close to the theoretical value calculated from Tanford's equation (Tanford et al. 1966). Dimensions of the chemically unfolded NADH oxidase are somewhat lower than the theoretical value, probably due to: i) differences in the primary structure (e.g. the number of glycine residues since glycine significantly contributes to the magnitude of the random coil viscosity (Tanford 1968)) and ii) residual structural elements in the monomeric unfolded state.

Discussion

In the present study, functional and structural properties of NOX in the dependence of pH have been studied by various biophysical and biochemical methods. Obtained results indicate on both local and global structural properties of the enzyme. Decreased pH resulted in a bell-shaped pH dependent transition of the catalytic rate constant (k_{cat}) of NOX from *T. thermophilus*. The different protonated states of NOX related to enzyme activity are summarized in Figure 7. Lowering the pH

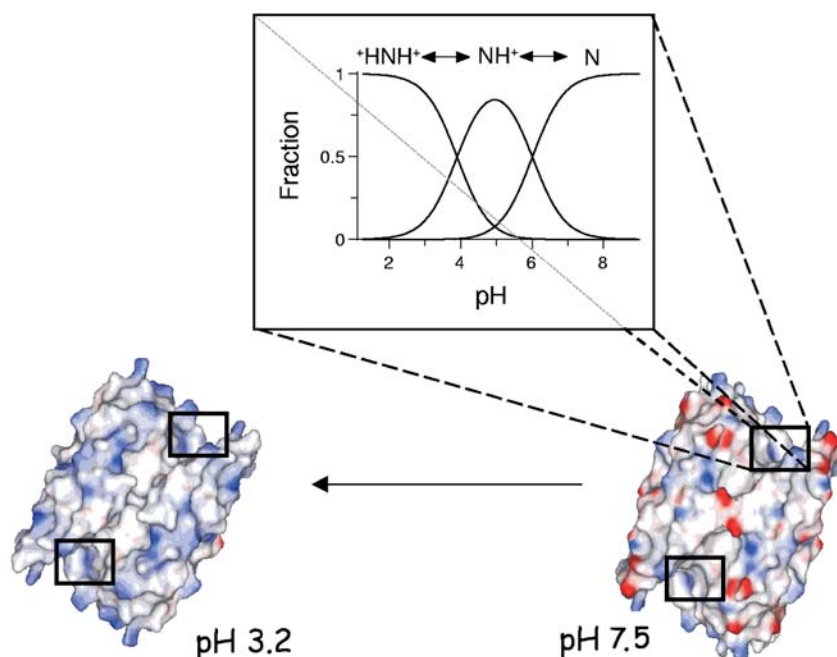


Figure 7. The change of surface electrostatic potential of NOX due to change in pH value. Squares indicate localization of active sites in the enzyme. Red and blue colors indicate negative and positive electrostatic potentials, respectively. Calculation of electrostatic potentials at different pH's was based on assumption of normal values of pK_a constants of side chains. Inset: The fractions of protonated and unprotonated species of NOX related to the enzyme activity (state of the active site) dependent on pH are shown. The fractions of the protonated (NH^+ , $+HNH^+$) and unprotonated (N) species of NOX were calculated according to the Eq. (8), based on parameters obtained from Figures 1 and 2.

from neutral to ~ 5.2 revealed protonation of a group with $pK_a \sim 6.0 \pm 0.1$. This transition was accompanied by about a 2-fold increase in the catalytic rate constant (Figure 1A, Table 1), and by a decrease in both the activation entropy and enthalpy (Figure 1B). Neither the intrinsic tryptophan fluorescence nor the ellipticity of the enzyme were significantly affected by the pH (Figure 1C), suggesting that the pH-induced structural alterations are very small.

The flavin system *re*-side is formed by Trp47 that stabilizes the position of the isoalloxazine ring through hydrogen bonds with a molecule of structural water – Wat42 (Hecht et al. 1995). The flavin ring *si*-side is formed by amino acid residues that stabilize the oxidized isoalloxazine ring with hydrogen bonds, i.e. Arg21 with the isoalloxazine N1/C2 positions and Gln73 with the N3 position (Figure 4). The pH-induced activation with $pK_a \sim 6.0$ strongly indicates participation of the histidine residue in the observed transition. Within 10 Å of the N1/N3 positions, there is only one amino acid residue that has a side chain with $pK_a \sim 6.0$. His75 is at a

distance of 5.88 and 4.64 Å from the N1 and N3 positions of the flavin ring, respectively. The other relatively close histidine is His101 at a distance of ~11 Å from the isoalloxazine N1/N3 positions, but localized within a second monomer. There are 4 histidines *per* monomer (75, 95, 101 and 194) but only His75 is from the same monomer as the flavin cofactor and this is a good candidate to be involved in regulation of NOX activity. Interestingly, in nitroreductase from *Vibrio fischeri*, His76 is in a similar position and at a similar distance (~6 Å; Koike et al. 1998). There are also a few examples of flavoenzymes with histidine residues of unknown function localized ~10 Å from the isoalloxazine ring: nitroreductases from *Escherichia coli* (Kobori et al. 2001), *Enterobacter cloacae* (Haynes et al. 2002) and NOX from *Streptococcus faecalis* (Ahmed and Claiborne 1992). It is quite possible that they all play a similar regulatory role.

It is noteworthy that ionization constants of protein groups can be highly perturbed. For example, in chicken lysozyme, the hydrophobic environment of Trp108 together with the electrostatic interaction of Asp52 contributes to the highly perturbed $pK_a \sim 6.1$ of Glu35 (Inoue et al. 1992). Acetoacetate decarboxylase has a highly perturbed amino group ϵNH_2 of Lys115 with $pK_a \sim 6.0$ due to its spatial proximity to the ϵNH_2 group of Lys116 (Schmidt and Westheimer 1971; Highbarger 1996). Therefore, a group with $pK_a \sim 6.0$, as detected in the present work, might be attributed to various groups with an abnormal pK_a . However, there are no aspartate, glutamate, cysteine or lysine residues within a 10 Å radius of the active site (N5 of the isoalloxazine ring). Thus, we conclude that protonation of the imidazole ring of His75 results in the observed pH dependent activity.

The protein structure at pH ~5.2 is very similar or the same as the native conformation at pH 7.5. This conclusion is based on the similar intrinsic viscosity, similar ellipticity in the peptide region, and similarity in the apparent transition temperature (91.4 and 87.6°C for pH 7.5 and 5.3, respectively). The question remains how does protonation of His75 affect NOX activity? The role of histidine residues located in close proximity to certain flavoenzyme active sites has been intensively studied (Su and Klinman 1999; Roth and Klinman 2003). An example of such an enzyme is glucose oxidase with His516, within ~4 Å of the isoalloxazine N1/N3 positions. This histidine is conserved within a group of several glucose, alcohol and cholesterol oxidases (Su and Klinman 1999). Lowering the pH results in an increased glucose oxidase rate constant despite a less favorable flavin redox potential for electron donation at low pH rather than high pH (Voet et al. 1981; Stankovich 1991). It has been concluded that protonated His516 accelerates the rate constant for the one electron transfer to dioxygen through electrostatic stabilization of the superoxide anion intermediate (Su and Klinman 1999). The catalytic cycle of most flavoproteins involves both FAD and FADH₂. Protonation of the protein moiety could differently affect the interaction between FAD and FADH₂. Moreover, the N1 position of the reduced flavin has a $pK_a = 6.7$ in solution (Muller 1991) and the observed pH activity profile could reflect ionization of the reduced flavin as opposed to the active site histidine. On the other hand, NMR studies of the reduced flavin in glucose oxidase from *Aspergillus niger* indicate that the N1 position of the

cofactor is perturbed, and is anionic even at pH 5.6 (Sanner et al. 1991). Speculation as to whether the protonated His75 in the NOX active site increases the NOX rate constant in a way similar to glucose oxidase from *A. niger*, i.e. through electrostatic stabilization of the anionic form of the flavin cofactor, remains an open question for future investigations. The fact that the oxidized flavin cofactor “recognizes” the presence of a group with a $pK_a \sim 6.0$, i.e. in the pH region where the oxidized flavin does not have a pH-induced transition, strongly indicates that the protein matrix is directly involved in the observed activity increase in NOX. The pH dependence of the k_{cat} and $k_{cat}/K_{M,app}$ (Table 1) is complex because they are followed by the protonation of enzyme-substrate, enzyme and the free substrate, respectively (Fersht 1999).

Several other amino acid residues in the NOX active site have probably a universal function common to nonhomologous flavoenzymes. An aromatic amino acid such as Trp and/or Phe (Trp47 in NOX), in a non-optimal, parallel orientation with the isoalloxazine ring (Burley and Petsko 1988), possibly functions as a gate that opens after the arrival of the substrate (Koike et al. 1998; Hubbard et al. 2001) or whose opening is necessary for the flavin cofactor to bind with the apoenzyme (Murray et al. 2003). A positively charged residue, Arg or Lys (Arg21 in NOX) positioned close to the isoalloxazine in the N1/C2 position, stabilizes the reduced flavin (Mewies et al. 1996; Watanabe et al. 1998; Craig et al. 2001; Xu et al. 2001). These examples indicate that information obtained from studies of nonhomologous flavoproteins might, in certain cases apply to a broaden class of flavoproteins.

The pH-induced inhibition of NOX at low pH is a one proton transition with an apparent $pK_a = 4.0 \pm 0.1$. In the present work we found that lower pH caused: i) release of Trp47 quenching by the flavin cofactor; ii) protonation of the adenine moiety of the flavin cofactor; iii) a slight perturbation of the secondary structure of NOX (~ 20 – 25% decrease in ellipticity at 222 nm); iv) dissociation of the flavin cofactor without affecting the quaternary structure of NOX; and v) decrease of the protein structure stability.

Dissociation of the flavin cofactor from the enzyme was accompanied by disappearance of the positive Cotton effect in the aromatic region of the circular dichroism spectrum as well as an increase in the cofactor fluorescence with $pK_a = 4.02 \pm 0.15$ and 3.94 ± 0.09 , respectively. The intrinsic tryptophan fluorescence increased in a sigmoidal transition with an apparent $pK_a = 3.85 \pm 0.07$ despite the finding that fluorescence of N-acetyl-L-tryptophanamide has no pH-induced transition in the pH region from 10 to 2 (Figure 2). These results support our suggestion that energy transfer from Trp47 to the flavin is similar to that observed in the glucose oxidase active site (Haouz et al. 1998). The energy transfer between Trp47 and the flavin cofactor also explains its low quantum yield at neutral pH (Žoldák et al. 2003) and its increase after the dissociation of cofactor (Figure 1C).

The lack of a pH-dependent transition of FMN indicates a major role of adenine protonation in the pH-induced changes of FAD fluorescence. In fact, only N1 of the adenine purine ring has an apparent pK_a ($pK_a \sim 3.9$) within the pH region between 5 and 2 (Peral and Gallego 2000). The apparent pK_a of the pH-induced

transition of free FAD fluorescence is 3.85 ± 0.07 suggesting a close interaction of the isoalloxazine and the adenine rings. Resonance energy transfer between these parts of the flavin moiety is not possible since the principal requirement for energy transfer, an overlap of adenine ring absorbance with the isoalloxazine ring emission spectrum does not exist. The FAD fluorescence is, therefore, quenched due to close proximity of the adenine and isoalloxazine ring in the intramolecular complex in solution (Weber 1950; van den Berg et al. 2002). A somewhat similar situation was described for NADH in solvent (Smith and Tanner 2000; Hull et al. 2001).

The apparent tendency of FAD in solution to achieve a folded conformation might partially explain the difference between dissociation constants of the FAD and FMN cofactors in NOX from *T. thermophilus* (1×10^{-5} mol/l and 9×10^{-8} mol/l, respectively (Hecht et al. 1995)). Binding of the FMN moiety of the FAD cofactor is essentially identical to that of FMN alone (Hecht et al. 1995). The unfolding of the FAD structure, as a necessary step for binding to the enzyme, might decrease the dissociation constant. There are no negatively charged amino acids in close proximity (10 Å radius) to the isoalloxazine ring. The excess of positive charge makes the active site of the apoenzyme cationic (Figure 7) with a total charge of $\sim +3$ at pH 7.0, assuming a normal pK_a of the titratable groups. Therefore, protonation of the adenine moiety, at pH < 4 , is very likely, to cause dissociation of FAD from the enzyme due to the repulsive electrostatic interactions of the positively charged amino acid residues, Arg17, Arg18, Arg195, and His194 located around the phosphate groups of the flavin cofactor.

Finally, using a combination of sedimentation velocity and sedimentation equilibrium we have shown that NOX from *T. thermophilus* is a stable dimer in the buffer within the pH range of 7.5 to 3.2. The sedimentation equilibrium distribution of enzyme in neutral pH buffer could be described as a single homogeneous species of molecular weight of $\sim 44,000$ Da. This value is consistent with a dimeric molecular weight of 45,400 Da as determined from the amino acid composition (Hecht et al. 1995). The stability of the NOX dimeric structure at different pH values was further analyzed by sedimentation velocity. In contrast to the chemically unfolded enzyme with $s_{20,w} = 1.5$ S, NOX at pH 7.5, 5.5 and 3.2 showed almost identical $s_{20,w} = 3.0$ S. Therefore, lowering of the pH did not result in dissociation of the dimeric quaternary structure of the apoform of NOX.

Acknowledgements. This work was supported by the Fonds der Chemischen Industrie, by the grants from the Deutsche Akademische Austauschdienst (DAAD, D/01/02768), the Slovak Grant Agency (1/0432/03), American Heart Association-Texas Affiliate (0465099Y to A. M.) and an internal grant from UPJS Faculty of Sciences (VVGs No. 427/2004 to G. Z. and M. S.). We thank Norbert Grillenbeck and Virgil Schirf (UTHSCSA) for technical assistance. The authors wish to thank Dr. LeAnn Robinson and Ms. Linda Sowdal for invaluable editorial help in preparing the manuscript.

References

- Acevedo O., Guzman-Casado M., Garcia-Mira M. M., Ibarra-Molero B., Sanchez-Ruiz J. M. (2002): pH corrections in chemical denaturant solutions. *Anal. Biochem.* **306**, 158—161
- Ahmed S. A., Claiborne A. (1992): Active-site structural comparison of streptococcal NADH peroxidase and NADH oxidase. Reconstitution with artificial flavins. *J. Biol. Chem.* **267**, 3832—3840
- Bánó M., Strhársky I., Hrmo I. (2003): A viscosity and density meter with a magnetically suspended rotor. *Rev. Sci. Instrum.* **74**, 4788—4793
- Burley S. K., Petsko G. A. (1988): Weakly polar interactions in proteins. *Adv. Protein Chem.* **39**, 125—189
- Cornish-Bowden A. (2002): Enthalpy-entropy compensation: a phantom phenomenon. *J. Biosci.* **27**, 121—126
- Craig D. H., Barna T., Moody P. C., Bruce N. C., Chapman S. K., Munro A. W., Scrutton N. S. (2001): Effects of environment on flavin reactivity in morphinone reductase: analysis of enzymes displaying differential charge near the N-1 atom and C-2 carbonyl region of the active-site flavin. *Biochem. J.* **359**, 315—323
- Dawson R. M. C., Elliott D. C., Elliott W. H., Jones K. M. (1986): Data for biochemical research. Oxford Science Publications
- Fersht A. (1999): Structure and Mechanism in Protein Science. pp. 175—176, W. H. Freeman and Company, New York
- Garcia-Mira M. M., Sanchez-Ruiz J. M. (2001): pH corrections and protein ionization in water/guanidinium chloride. *Biophys. J.* **81**, 3489—3502
- Haouz A., Twist C., Zentz C., de Kersabiec A.-M., Pin S., Alpert B. (1998): Förster energy transfer from tryptophan to flavin in glucose oxidase enzyme. *Chem. Phys. Lett.* **294**, 197—203
- Haynes C. A., Koder R. L., Miller A. F., Rodgers D. W. (2002): Structures of nitroreductase in three states: effects of inhibitor binding and reduction. *J. Biol. Chem.* **277**, 11513—11520
- Hecht H. J., Erdmann H., Park H. J., Sprinzl M., Schmid R. D. (1995): Crystal structure of NADH oxidase from *Thermus thermophilus*. *Nat. Struct. Biol.* **2**, 1109—1114
- Highbarger L. A., Gerlt J. A., Kenyon G. L. (1996): Mechanism of the reaction catalyzed by acetoacetate decarboxylase. Importance of lysine 116 in determining the p*K*_a of active-site lysine 115. *Biochemistry* **35**, 41—46
- Hubbard P. A., Shen A. L., Paschke R., Kasper C. B., Kim J. J. (2001): NADPH-cytochrome P450 oxidoreductase. Structural basis for hydride and electron transfer. *J. Biol. Chem.* **276**, 29163—29170
- Hull R. V., Conger P. S. 3rd, Hoobler R. J. (2001): Conformation of NADH studied by fluorescence excitation transfer spectroscopy. *Biophys. Chem.* **90**, 9—16
- Kengen S. W., van der Oost J., de Vos W. M. (2003): Molecular characterization of H₂O₂-forming NADH oxidases from *Archaeoglobus fulgidus*. *Eur. J. Biochem.* **270**, 2885—2894
- Kobori T., Sasaki H., Lee W. C., Zenno S., Saigo K., Murphy M. E., Tanokura M. (2001): Structure and site-directed mutagenesis of a flavoprotein from *Escherichia coli* that reduces nitro compounds: alteration of pyridine nucleotide binding by a single amino acid substitution. *J. Biol. Chem.* **276**, 2816—2823
- Koder R. L., Haynes C. A., Rodgers M. E., Rodgers D. W., Miller A. F. (2002): Flavin thermodynamics explain the oxygen insensitivity of enteric nitroreductases. *Biochemistry* **41**, 14197—14205

- Koike H., Sasaki H., Kobori T., Zenno S., Saigo K., Murphy M. E., Adman E. T., Tanokura M. (1998): 1.8 Å crystal structure of the major NAD(P)H : FMN oxidoreductase of a bioluminescent bacterium *Vibrio fischeri*: overall structure, cofactor and substrate-analog binding, and comparison with related flavoproteins. *J. Mol. Biol.* **280**, 259—273
- Inoue M., Yamada H., Yasukochi T., Kuroki R., Miki T., Horiuchi T., Imoto T. (1992): Multiple role of hydrophobicity of tryptophan-108 in chicken lysozyme: structural stability, saccharide binding ability, and abnormal pK_a of glutamic acid-35. *Biochemistry* **31**, 5545—5553
- Laemmli U. K. (1970): Cleavage of structural proteins during the assembly of the head of bacteriophage T4. *Nature* **227**, 680—685
- Liochev S. I., Hausladen A., Fridovich I. (1999): Nitroreductase A is regulated as a member of the soxRS regulon of *Escherichia coli*. *Proc. Natl. Acad. Sci. U.S.A.* **96**, 3537—3539
- Mewies M., Packman L. C., Mathews F. C., Scrutton N. S. (1996): Flavinylation in wild-type trimethylamine dehydrogenase and differentially charged mutant enzymes: a study of the protein environment around the N1 of the flavin isoalloxazine. *Biochem. J.* **317**, 267—272
- Muller F. (1991): *Chemistry and Biochemistry of Flavoenzymes*. pp. 1—72, CRC Press, Boca Raton, Florida
- Musatov A., Ortega-Lopez J., Robinson N. C. (2000): Detergent-solubilized bovine cytochrome *c* oxidase: dimerization depends on the amphiphilic environment. *Biochemistry* **39**, 12996—13004
- Murray T. A., Foster M. P., Swenson R. P. (2003): Mechanism of flavin mononucleotide cofactor binding to the *Desulfovibrio vulgaris* flavodoxin. 2. Evidence for cooperative conformational changes involving tryptophan 60 in the interaction between the phosphate- and ring-binding subsites. *Biochemistry* **42**, 2317—2327
- Pace C. N., Vajdos F., Fee L., Grimsley G., Gray T. (1995): How to measure and predict the molar absorption coefficient of a protein. *Protein Sci.* **4**, 2411—2423
- Park H. J., Kreutzer R., Reiser C. O. A., Sprinzl M. (1992): Molecular cloning and nucleotide sequence of the gene encoding a H₂O₂-forming NADH oxidase from the extreme thermophilic *Thermus thermophilus* HB8 and its expression in *Escherichia coli*. *Eur. J. Biochem.* **205**, 875—879
- Park H. J., Reiser C. O. A., Kondruweit S., Erdmann H., Schmid R. D., Sprinzl M. (1992): Purification and characterization of a NADH oxidase from the thermophile *Thermus thermophilus* HB8. *Eur. J. Biochem.* **205**, 881—885
- Parkinson G. N., Skelly J. V., Neidle S. (2000): Crystal structure of FMN-dependent nitroreductase from *Escherichia coli* B: a prodrug-activating enzyme. *J. Med. Chem.* **43**, 3624—3631
- Peral F., Gallego E. (2000): The self-organization of adenosine 5'-triphosphate and adenosine 5'-diphosphate in aqueous solution as determined from ultraviolet hypochromic effects. *Biophys. Chem.* **85**, 79—92
- Roth J. P., Klinman J. P. (2003): Catalysis of electron transfer during activation of O₂ by the flavoprotein glucose oxidase. *Proc. Natl. Acad. Sci. U.S.A.* **100**, 62—67
- Sanner C., Macheroux P., Ruterjans H., Muller F., Bacher A. (1991): 15N- and 13C-NMR investigations of glucose oxidase from *Aspergillus niger*. *Eur. J. Biochem.* **196**, 663—672
- Schmidt D. E. Jr., Westheimer F. H. (1971): pK of the lysine amino group at the active site of acetoacetate decarboxylase. *Biochemistry* **10**, 1249—1253
- Smith P. E., Tanner J. J. (2000): Conformations of nicotinamide adenine dinucleotide (NAD⁺) in various environments. *J. Mol. Recognit.* **13**, 27—34

- Stankovich M. T. (1991): Chemistry and Biochemistry of Flavoenzymes. pp. 401—425, CRC Press, Boca Raton, Florida
- Su Q., Klinman J. P. (1999): Nature of oxygen activation in glucose oxidase from *Aspergillus niger*: the importance of electrostatic stabilization in superoxide formation. *Biochemistry* **38**, 8572—8581
- Tanford C., Kawahara K., Lapanje S. (1966): Proteins in 6-M guanidine hydrochloride. Demonstration of random coil behavior. *J. Biol. Chem.* **241**, 1921—1923
- Tanford C. (1968): Protein denaturation. *Adv. Protein Chem.* **23**, 121—282
- van den Berg P. A. W., Feenstra K. A., Mark A. E., Berendsen H. J. C., Visser A. J. W. G. (2002): Dynamic conformations of flavin adenine dinucleotide: Simulated molecular dynamics of the flavin cofactor related to the time-resolved fluorescence characteristics. *J. Phys. Chem.* **106**, 8858—8869
- Voet J. G., Coe J., Epstein J., Matosian V., Shipley T. (1981): Electrostatic control of enzyme reactions: effect of ionic strength on the pK_a of an essential acidic group on glucose oxidase. *Biochemistry* **20**, 7182—7185
- Xu D., Ballou D. P., Massey V. (2001): Studies of the mechanism of phenol hydroxylase: mutants Tyr289Phe, Asp54Asn, and Arg281Met. *Biochemistry* **40**, 12369—12378
- Ward D. E., Donnelly C. J., Mullendore M. E., van der Oost J., de Vos W. M., Crane E. J. 3rd (2001): The NADH oxidase from *Pyrococcus furiosus*. Implications for the protection of anaerobic hyperthermophiles against oxidative stress. *Eur. J. Biochem.* **268**, 5816—5823
- Watanabe M., Nishini T., Takio K., Sofuni T., Nohmi T. (1998): Purification and characterization of wild-type and mutant “classical” nitroreductases of *Salmonella typhimurium*. *J. Biol. Chem.* **273**, 23922—23928
- Weber G. (1950): Fluorescence of riboflavin and flavin-adenine dinucleotide. *Biochem. J.* **47**, 114—121
- Wyman J., Gill S. J. (1990): Independent-site binding reactions. In: Binding and Linkage. Functional Chemistry of Biological Macromolecules. pp. 44—46. University science books, Mill Valley, California
- Žoldák G., Šuťák R., Antalík M., Sprinzl M., Sedlák E. (2003): Role of conformational flexibility for enzymatic activity in NADH oxidase from *Thermus thermophilus*. *Eur. J. Biochem.* **270**, 4887—4897
- Žoldák G., Sprinzl M., Sedlák E. (2004): Modulation of activity of NADH oxidase from *Thermus thermophilus* through change in flexibility in the enzyme active site induced by Hofmeister series anions. *Eur. J. Biochem.* **271**, 48—57